Architectural Control Syntheses of CdS and CdSe Nanoflowers, Branched Nanowires, and Nanotrees via a Solvothermal Approach in a Mixed Solution and Their Photocatalytic Property

Wei-Tang Yao, Shu-Hong Yu,* Shu-Juan Liu, Jun-Peng Chen, Xian-Ming Liu, and Fan-Qing Li

Division of Nanomaterials & Chemistry, Hefei National Laboratory for Physical Sciences at Microscale, School of Chemistry & Materials, Department of Chemistry, University of Science and Technology of China, Hefei 230026, P. R. China

Received: January 9, 2006; In Final Form: April 21, 2006

Wurtzite CdS and CdSe nanostructures with complex morphologies such as urchin-like CdS nanoflowers, branched nanowires, and fractal nanotrees can be produced via a facile solvothermal approach in a mixed solution made of diethylenetriamine (DETA) and deionized water (DIW). The morphologies of CdS and CdSe nanocrystals can be easily controlled via tuning the volume ratio of DETA and DIW. Urchin-like CdS nanoflowers made of CdS nanorods are in a form of highly ordered hierarchical structures, while the nanowires are branched nanowires, and the fractal CdS nanotrees are a buildup of branched nanopines. The results demonstrated that solvothermal reaction in a mixed amine/water can access a variety of complex morphologies of semiconductor materials. The photocatalytic activity of CdS particles with different morphologies has been tested by the degradation of *acid fuchsine* under both UV and visible light, showing that the as-prepared branched CdS nanowires exhibit high photocatalytic activity for degradation of *acid fuchsine*.

Introduction

As one of the most vital and classical II−VI group semiconductors, synthesis of CdS has been extensively explored during the past decades. It is a well-studied semiconductor with a direct band gap of 2.4 eV at room temperature, and it is now widely used for photoelectric conversion in solar cells, in light-emitting diodes for flat-panel displays, and in other optical devices based on its nonlinear properties.[1] Over the past few years, tremendous effort has been made to control the size and shape of CdS nanocrystals, and a huge number of new methods have been reported for the synthesis of CdS-based nanostructures, especially one-dimensional CdS nano- or microstructures. For instance, high-quality CdS nanocrystals can be synthesized by use of tri-*n*-octylphosphine oxide (TOPO) or hexadecylamine (HDA) as a shape-controlling capping ligand and a stabilizing ligand, which were explored by Alivisatos, Peng, and other groups.[2] Lieber and his colleagues have fabricated thin CdS nanowires by laser ablation of CdS and a metal catalyst mixed target.[1d,e] Solution-based routes with or without organic surfactants and high temperature thermal decomposition or chemical vapor deposition (CVD) methods were also developed rapidly to synthesize one-dimensional CdS nanostructures such as nanorods,[3] nanowires,[4] nanotubes,[5] and nanobelts.[6] In addition, CdS and CdSe nanorods/nanowires can also be prepared via a solvothermal approach with use of ethylenediamine as template.[7]

Although various architectures with nanometer- and micrometer-sized dimensions have been observed for the above-mentioned nanostructures in solution-based processes, synthesis of complex structures (such as bipod, tretrapod, multi-arm CdS nanostructures) made of CdS nanocrystals is rarely reported.[2d,e,3g] Conceptually, branched nanowires offer a novel route for increasing structural complexity and endowing greater function.[8] Branched nanocrystals, nanowires, and nanoribbon structures have been reported previously.[9] Tetrapod-shaped cadmium telluride (CdTe) nanostructures also have been synthesized by Alivisatos and colleagues.[9a] Other complex oxide structures such as tadpole-like ZnO branch nanoarrys[9b] and hierarchical ZnO branch nanostructures with 6-, 4-, and 2-fold symmetries can be synthesized through a vapor−liquid−solid process or a vapor transport and condensation technique.[9c] All these show the possibility to access unique nanostructures with complexity, which may drive some unique and exciting applications. Thus, how to design and develop new solution-based methods to prepare novel CdS nanostructures and other similar semiconductors is still one of the most important tasks at present.

Previously, two-phase heterogeneous solution media has been developed for the synthesis of noble metal nanoparticles[10] and CdS nanoparticles.[11] Recently, our group has introduced a solvothermal reaction in a homogeneous mixed solution to synthesize ZnS nanobelts,[12] complex wurtzite ZnSe microspheres with hierarchical fractal structure,[13] and inorganic−organic hybrid $[ZnSe](DETA)_{0.5}$ nanobelts.[14] Herein, novel and complex CdS and CdSe nanostructures with flower-like, wire-like, and tree-like structures have been synthesized via a solvothermal method with use of a mixed solution made of diethylenetriamine (DETA) and deionized water (DIW). The photocatalytic activity of these complex nanostructures for degradation of acid fuchsine has been investigated.

Experimental Section

Preparation of CdE (E = S, Se) Nanostructures. All chemicals are analytical grade and are used as received without further purification. In a typical procedure, 0.266 g of Cd(Ac)

* Address correspondence to this author. Fax: + 86 551 3603040. E-mail: shyu@ustc.edu.cn.

10.1021/jp060164n CCC: $33.50
Published on Web 05/27/2006

$_2$·$2H_2O$ (~1 mmol) and 0.076 g of CS $(NH_2)_2$ (~1 mmol) or 0.173 g of Na_2SeO_3 (~1 mmol) were added into a mixed solution of diethylenetriamine (DETA) and deionized water (DIW) with different volume ratios. The mixed solution was then transferred into to a Teflon-lined autoclave (at its 80% capacity of a total 50 mL). The autoclave was sealed and kept at 180 °C for 12 h, and then cooled to room temperature naturally. After the reaction, the solution was filtered and washed by deionized water and absolute ethanol, and the product was dried in a vacuum at 80 °C for 6 h.

Photocatalytic Activity Measurement. A cylindrical Pyrex flask (capacity ca. 25 mL) was used as the photoreactor vessel. The reaction system containing acid fuchsine ($C_{20}H_{17}N_3O_9S_3$-Na_2) (Sigma-Aldrich Chemical Co.; 5.0×10^{-5} M, 20 mL) and CdS nanoparticles as catalyst (10 mg) was magnetically stirred in the dark for 5 min to reach the adsorption equilibrium of acid fuchsine with the catalyst, and then exposed to light from a Philips HPK high-pressure Hg lamp (125 W). Commercial TiO_2 (Degussa P25, Degussa Co.) was adopted as the reference with which to compare the photocatalytic activity under the same experimental conditions. UV−vis absorption spectra were recorded at different intervals to monitor the reaction.

Characterization. Transmission electron microscope (TEM) photographs were taken on a Hitachi Model H-800 transmission electron microscope at an accelerating voltage of 200 kV. The morphologies and sizes of the samples were examined by field emission scanning electron microscopy (FESEM, JEOL JSM-6700F, operated at 10 kV). Element analysis was conducted by energy-dispersive spectra (EDS) on a JEOL JSM 6700 scanning electron microanalyzer (SEM). High-resolution transmission electron microscope (HRTEM) photographs and selected area electron diffraction (SAED) patterns were performed on a JEOL-2010 transmission electron microscope. Energy-dispersive X-ray (EDX) analysis was also done with a JEOL-2010 transmission electron microscope with an Oxford windowless Si (Li) detector equipped with a 4 pulse processor. This detector enables elemental identification down to boron, on areas as small as 1 nm^2 and with typically ~140 eV resolution. UV−vis spectra were recorded on a Shimadzu UV-240 spectrophotometer at room temperature.

Results and Discussion

Structure and Morphology. Figure 1 shows that the XRD patterns of the products obtained after reaction at 180 °C for 12 h in a mixed solution with different volume ratios of DETA and DIW. All the diffraction peaks can be indexed as pure hexagonal wurtzite CdS with cell parameters $a = 4.14$ Å and $b = 6.72$ Å, which are consistent with the literature values (JCPDS card number 41-1049). However, the relative intensity of the peaks corresponding to the (002)/(100) and (002)/(101) planes varied significantly from the literature values, indicating the possible special tropism of the products.

The morphology and size of the products were examined by FESEM and TEM. Figure 2a shows that the product consists of relatively uniform urchin-like CdS nanoflowers with an average size of 3.5 μm synthesized in a mixed solution with a volume ratio of V_{DETA}:V_{DIW} of 2:5. It is interesting that each nanoflower is made up of many CdS nanorods aligned in a radial way (Figure 2b) (see also the Supporting Information, Figure S1). Energy-dispersive spectra (EDS) analysis of nanoflowers (Figure 2c) indicated the molar ratio of Cd and S is 1.013:1, which was close to that of the stoichiometric composition. Due to the use of Al foils as the samples substrate, the signal from Al element was observed in the EDS spectrum. Increasing the

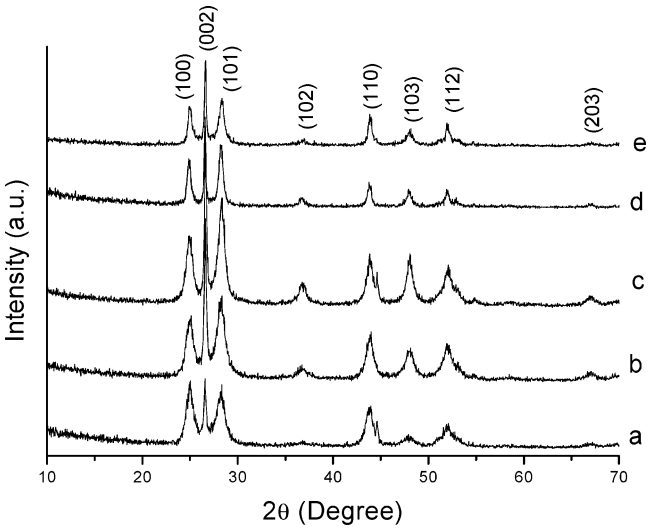

Figure 1. XRD patterns of the product obtained after reaction at 180 °C for 12 h in mixed solutions with different volume ratios of V_{DETA}:V_{DIW}: (a) 33:2; (b) 6:1; (c) 1:1; (d) 2:5; and (e) 1:6.

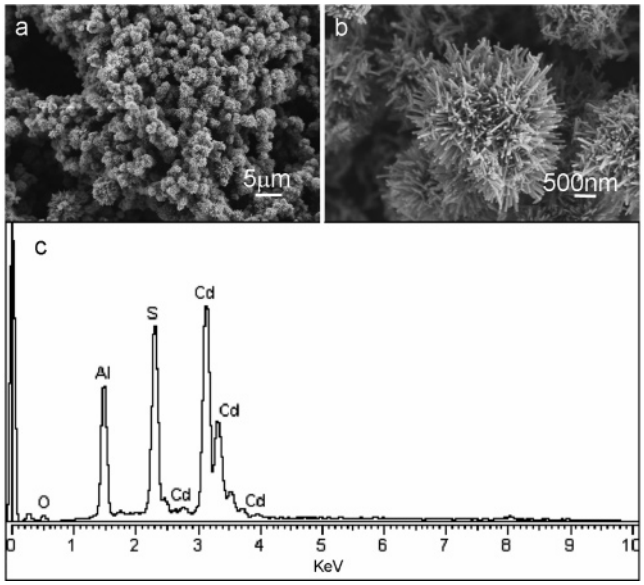

Figure 2. FE-SEM images of the product prepared at 180 °C for 12 h. V_{DETA}:V_{DIW} = 2:5: (a) low-magnification image and (b) a typical single CdS nanoflower. (c) The corresponding EDS spectrum taken from the CdS nanoflowers shown in part a.

volume ratio of V_{DETA}:V_{DIW} in this reaction system can change the morphology gradually. Interestingly, wire-like hierarchical CdS structures made of branched nanowires formed when the volume ratio reached 6:1 (Figure 3). Figure 3a,b shows that the CdS nanostructures are made up of CdS branched nanowires and some CdS branched nanowire arrays can also be observed (Figure 3b). Figure 3c,d shows a typical dendritic CdS particle made of branched nanowires. Energy-dispersive X-ray (EDX) analysis on the branched CdS nanowires suggested that the molar ratio of the sample is 1.074:1 (Figure 3e), which was near the standard stoichiometric composition. Both EDS and EDX analysis on such CdS nanostructures indicated that Cd element is a little bit in excess of S element in the sample, which is consistent with the result by XPS (see the Supporting Information, Figure S3).

To investigate the effect of an additional capping ligand or a surfactant on the CdS nanostructures in the present system, a suitable amount of hexadecylamine (HDA) was added to the present preparation system. Surprisingly, branched CdS nanow-

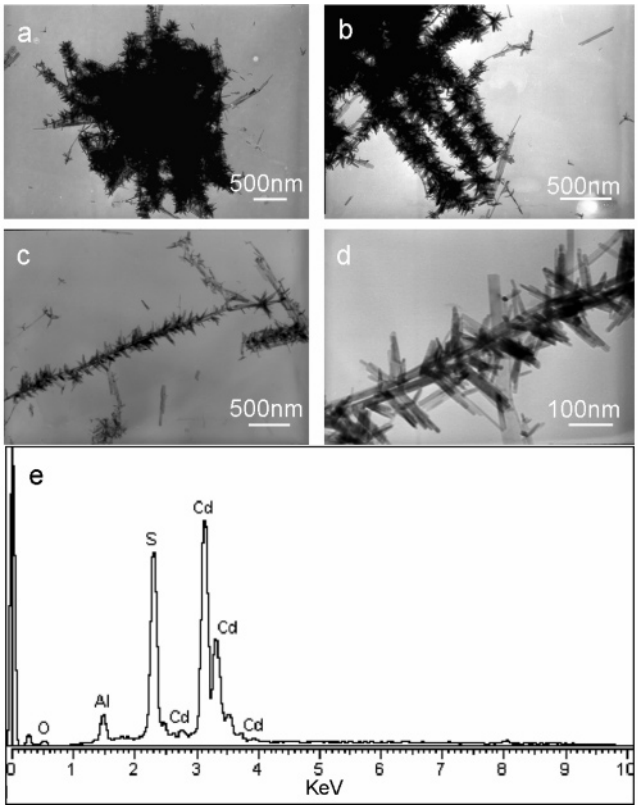

Figure 3. TEM images of the products obtained after reaction at 180 °C for 12 h. V_{DETA}:V_{DIW} = 6:1: (a and b) low-magnification images, (c) a typical single branched CdS nanowire, and (d) partial magnified image of part c. (e) The corresponding EDX spectrum taken from the branched CdS nanowires shown in part b.

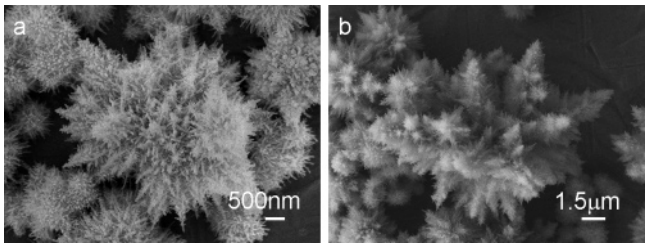

Figure 4. FE-SEM images of the products prepared at 180 °C for 12 h. V_{DETA}:V_{DIW} = 6:1; 1.2 g of HAD was added in this reaction solution. (a) A magnified image of fractal CdS nanotrees and (b) a general overview image.

ires cannot be obtained, instead, tree-like with fractal structure CdS microtrees formed (Figure 4). This phenomenon is similar to that of CdSe fractal nanocrystals reported by Li and co-workers;[7b] however, there are some differences. The CdS nanotrees produced here were found to be made up of many branched nanopines with different growth directions and displayed high hyperbranched nanostructures, which are similar to the three-dimensional hyperbranched CdTe and CdSe reported recently by Alivisatos.[15] The exact mechanism for the formation of fractal structure CdS nanotrees is still unclear at present. However, diffusion-limited aggregation (DLA)[16] and nucleation-limited aggregation (NLA) models[17] could be used to interpret the formation of such complex CdS fractal nanotrees.

TEM images in Figure 5a,b reveal that the CdS nanoflowers are composed of densely branched nanorods with a diameter of 30−40 nm. Figure 5c shows a typical nanorod with a diameter of 30−40 nm and length about 150 nm-460 nm with a single crystalline nature as shown in the insert electron diffraction pattern (ED). High-resolution TEM (HRTEM) images in Figure 5d,e show that the nanorod has clear lattice fringes with a lattice spacing of about 3.4 Å, corresponding to the spacing for the (002) planes of wurtzite CdS, which is consistent with that by the ED pattern (inset in Figure 5c). The results demonstrated that the nanorods grow along the [002] direction (Figure 5e).

Figure 6a,b shows a typical wire-like particle made of branched CdS nanowires. Figure 6b shows that each branch has an angle with a trunk about 83.5° from the primary direction. High-resolution transmission electron microscopy (HRTEM) images show clearly the obvious stacking faults within knots between the branches and the nanowires. This behavior is well-known to be due to the small energy difference between stacking sequences in this growth direction.[3h,18] The trunk has clear lattice spacing of about 3.4 Å corresponding to the spacing for the (002) planes of wurtzite CdS and the preferential [002] growth direction. It is fantastic that the trunk of CdS branched nanowires always grew along the same direction [002]. It is different from some other CdE (E = S, Se, or Te) branched nanocrystals or mutilpod structures, whose central core usually belongs to cubic structure and the branch (or arm) is hexagonal nanostructures as reported by Peng, Alivisatos, and other groups.[9a,18b]

The influence of the volume ratio of DETA and DIW on the formation of CdS nanostructures was investigated. When the volume ratio of DETA and DIW reached 1:6, all the particles were in a form of microspheres built up by shorter and thicker CdS nanorods (Figure 7a,b). Particles comprised of cage-like microspheres with a size ranging from 3 to 4 μm were obtained if the volume ratio of DETA and DIW was kept as 1:1 (Figure 7c,d). These microspheres are composed of densely disordered thicker nanorods (Figure 7d), which are different from the urchin-like CdS nanoflowers, or branched nanowires, or fractal structure CdS nanotrees as shown in Figures 2a,b, 3a,b, and 4a,b, respectively.

It is worth mentioning that the morphologies of CdS change subtly with a gradual increase of the volume ratio of DETA and DIW, suggesting that the volume ratio of DETA and DIW plays a key role in the formation of diverse CdS nanostructures, such as CdS nanoflowers, branched nanowires, and nanotrees (Figures 2a,b, 3a,b, and 4a,b). In addition, CdSe nanoflowers and multiarm nanostructures can also be synthesized in a similar mixed solution by a solvothermal process (Figure 8, see also the Supporting Information, Figure S2), indicating the universality and versatility of this new reaction medium for controlling the morphology of a family of semiconductor nanostructures. The EDS analysis indicated the composition of the sample was $Cd_{1.42}Se$.

Optical Properties of CdS Nanostructures. The optical properties of these nanomaterials with complex form display strong quantum-size effects compared with those of the bulk materials. The UV−vis absorption spectra for the samples synthesized in the present mixed solution with different volume ratios of V_{DETA}:V_{DIW} are shown in Figure 9. All the products display a broad absorption peak in the range of 450−500 nm with a central peak position at about 486 (2.55 eV), 482 (2.57 eV), 477 (2.60 eV), 475 (2.61 eV), 474 (2.62 eV), and 488 nm (2.54 eV), respectively (Figure 9a−f), which are all shifted toward high energy compared with the bulk CdS.[1] This feature is consistent with that observed previously in the case of CdS nanoparticles and nanorods.[19] In addition, in the sample obtained in the mixed solution with a volume ratio of V_{DETA}:V_{DIW} = 1:6, an additional adsorption peak located at 280 nm was observed (curve f in Figure 9)—its origin is still not clear.

Photocatalytic Activity Properties of CdS Nanostructures. It is well-known that CdS has been used as a semiconductor-

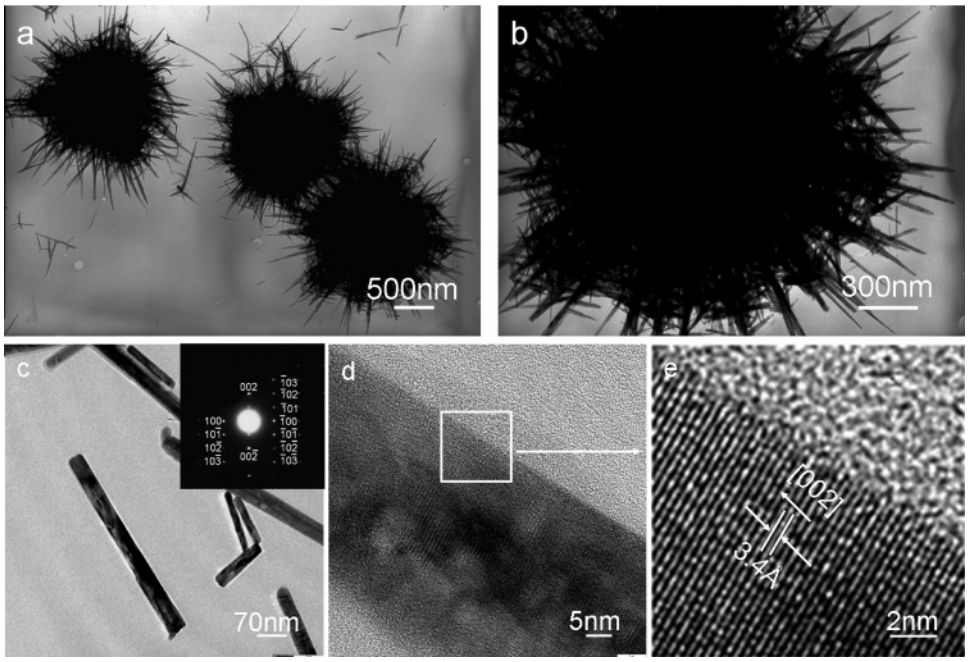

Figure 5. (a, b) TEM and (c, d, e) HRTEM images of the products prepared at 180 °C for 12 h. V_{DETA}:V_{DIW} = 2:5. The inset of part c is the corresponding SAED pattern taken from a singe CdS nanorod of part c.

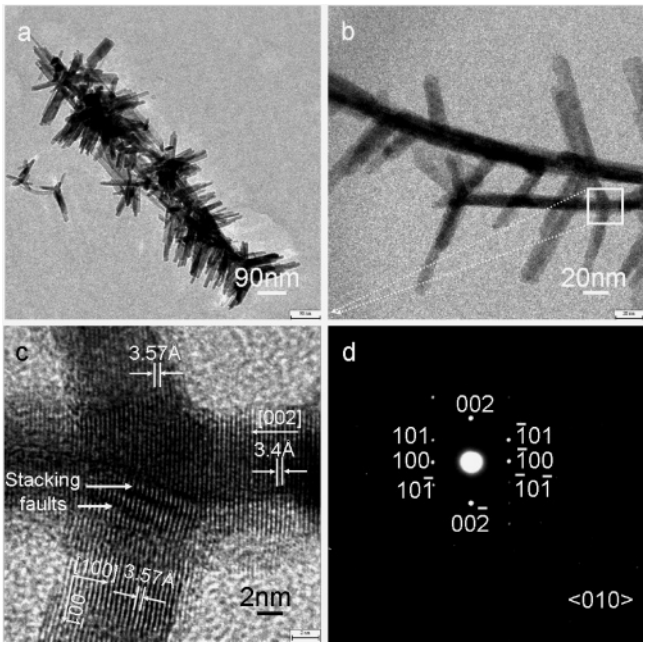

Figure 6. (a, b) TEM and (c) HRTEM images of the products prepared at 180 °C for 12 h. V_{DETA}:V_{DIW} = 6:1. (d) SAED pattern taken from the trunk of the CdS branched nanowire of part b.

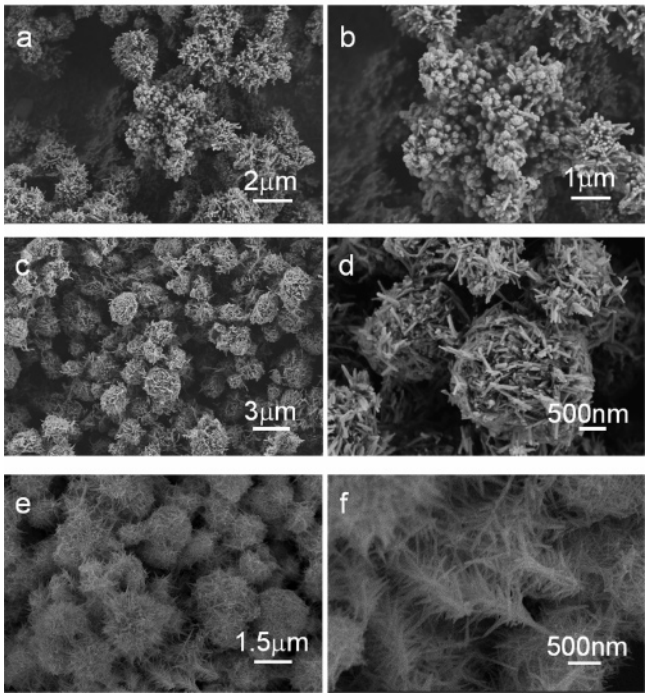

Figure 7. FE-SEM images of the products prepared at 180 °C for 12 h: (a, b) V_{DETA}:V_{DIW} = 1:6, (c, d) V_{DETA}:V_{DIW} = 1:1, (e, f) V_{DETA}:V_{DIW} = 25:10.

type photocatalyst for the photoreductive dehalogenation of halogenated benzene derivatives, photocatalytic degradation of water pollutants, and photocatalytic reduction of toxic metal ions.[20,21] To demonstrate the potential applicability of as-synthesized CdS nanomaterials in these applications, we investigated their photocatalytic activity by choosing photocatalytic degradation of acid fuchsine as a test reaction. The characteristic absorption of acid fuchsine at about 543 nm was chosen as the monitored parameter for the photocatalytic degradation process. Figure 10 shows the absorption spectra of an aqueous solution of acid fuchsine (initial concentration: 5.0×10^{-5} M, 20 mL) in the presence of 10 mg CdS nanoparticles prepared under different conditions under exposure to UV light for 40 min. The absorption peaks corresponding to the acid fuchsine, such as the sharp peak at 543 nm, almost diminish gradually as the exposure time increases, and completely disappear after about 40 min. No new absorption bands appear in either the visible or ultraviolet regions, suggesting the complete photodegradation of acid fuchsine. The final results indicated that the photocatalytic activity of branched CdS nanowires prepared in a mixed solution with a volume ratio of V_{DETA}:V_{DIW} of 6:1 is highest among all kinds of CdS nanostructures prepared in the present reaction system.

To understand the potential advantage of branched CdS nanowires as photodegradation nanomaterials, time-dependent UV−vis absorption spectra of photocatalysis degraded acid

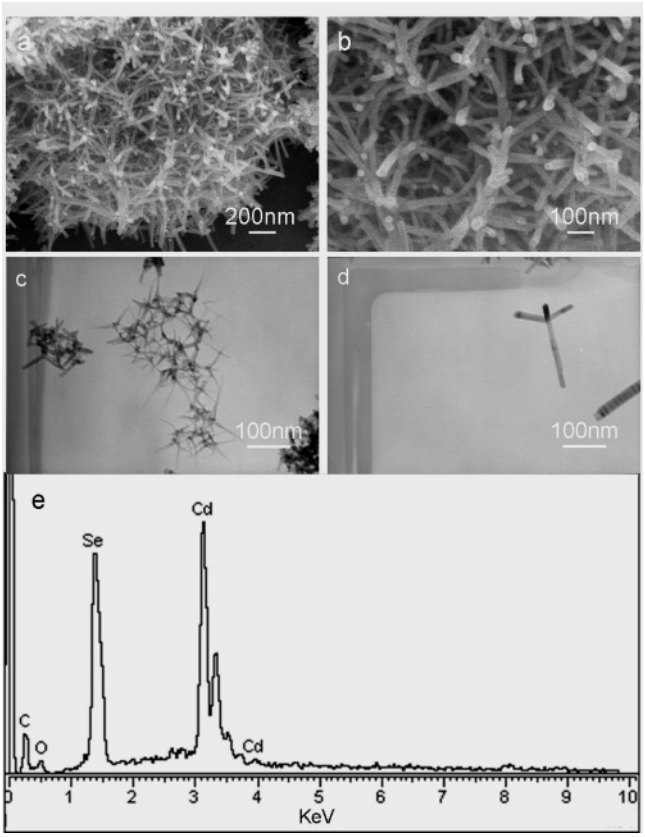

Figure 8. FE-SEM (a, b) and TEM images (c, d) of CdSe nanostructures prepared at 180 °C for 12 h, V_{DETA}:V_{DIW} = 6:1. (e) The corresponding EDX spectrum taken on the CdS nanostructures shown in part a.

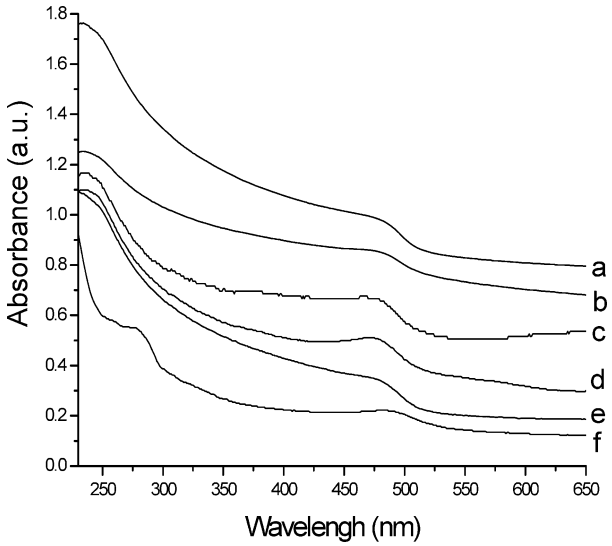

Figure 9. The UV−vis absorption spectra of the products prepared at 180 °C for 12 h in a mixed solution with different volume ratios of V_{DETA}:V_{DIW}: (a) 33:2; (b) 6:1; (c) 25:10; (d) 1:1; (e) 10:25; and (f) 1:6.

fuchsine were recorded (bottom part in Figure 11). As shown in Figure 11, the absorbance intensity for the peak at 543 nm decreases very quickly once the branched CdS nanowires were added, corresponding to the immediate color change. The results suggested that the branched CdS nanowires may have a high BET surface and thus can adsorb the dye molecules more efficiently. With exposure time increasing, the typical sharp peak at 543 nm diminished gradually and completely vanished after 45 min. A series of color changes (upper part in Figure 11)

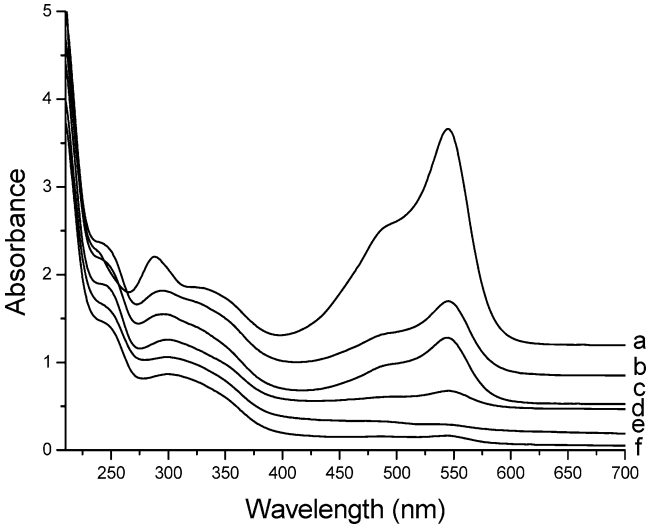

Figure 10. The absorption spectra of a solution of acid fuchsine (5×10^{-5} M, 20 mL) in the presence of CdS nanoparticles (10 mg) under exposure to UV light for 40 min: (a) initial acid fuchsine solution; (b−f) corresponding to the spectra measured after adding the samples prepared in mixed solution with different volume ratios of V_{DETA}:V_{DIW} of (b) 33:2, (c) 1:6, (d) 2:5, (e) 1:1, and (f) 6:1.

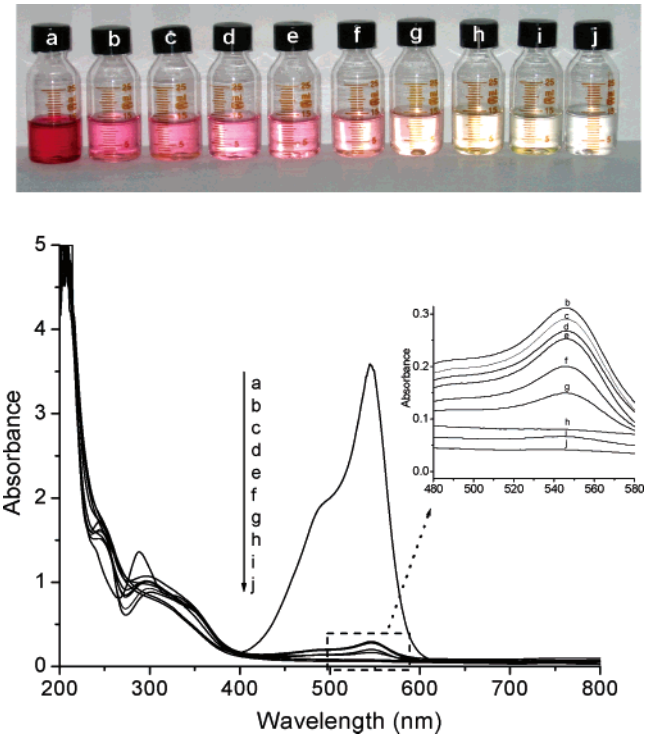

Figure 11. Time-dependent color change (see the picture in the upper part) and corresponding time-dependent absorption spectra of a solution of acid fuchsine (5×10^{-5} M, 20 mL) in the presence of branched CdS nanowires after its exposure to UV light (the down part): (a) initial solution; (b) after adding the CdS nanowires; and (c−j) after exposure to UV light for (c) 5, (d) 15, (e) 30, (f) 45, (g) 75, (h) 125, (i) 175, and (j) 235 min. The inset shows the enlarged temporal evolution of absorption (b−j).

correspond to the sequential changes detected by the UV−vis absorption measurements

The nitrogen adsorption−desorption isotherm of branched CdS nanowires was investigated (Figure 12a). The Brunauer−Emmett−Teller (BET) surface area is 58.7 m^2/g, and the Barrett−Joyner−Halenda (BJH) calculations for the pore-size distribution, derived from desorption data, reveal a distribution centered at 4.6 nm (Figure 12b). The Barrett−Joyner−Halenda

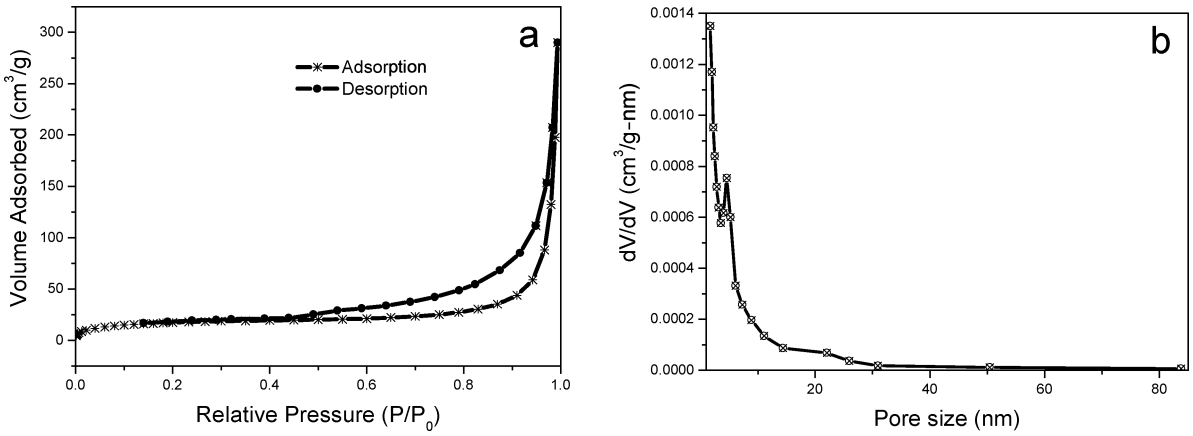

Figure 12. (a) Typical N_2 gas adsorption−desorption isotherm of branched CdS nanowires and (b) pore size distribution.

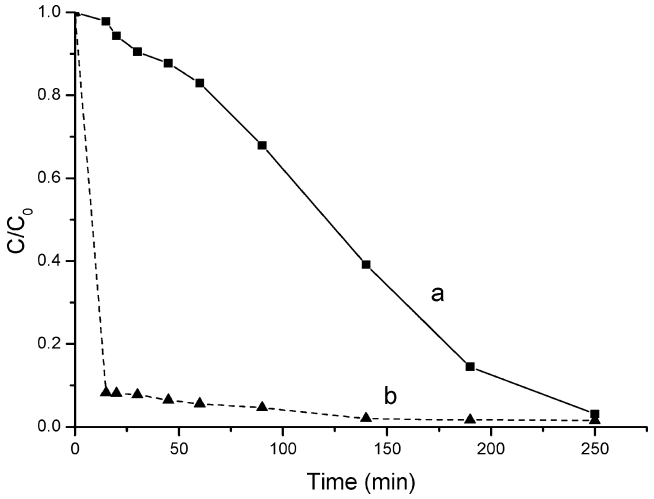

Figure 13. Photodegradation of acid fuchsine (5×10^{-5} M, 20 mL) under different conditions: (a) with Degussa P25 titania (10 mg) and UV light and (b) with branched CdS nanowires (10 mg) and UV light.

(BJH) adsorption/desorption average pore diameter is 5.8/4.7 nm. The branched CdS nanowires are of larger specific surface area than that of Degussa P25 powder (the surface area of Degussa P25 powder is ca. 45 m^2/g[22]), and hence could show stronger adsorption to acid fuchsine molecules.

Further experiments were carried out to compare the catalytic activity of the branched CdS nanowires with Degussa P25 titania. Degussa P25 titania (10 mg) and branched CdS nanowires (10 mg) were added into two identical solutions of acid fuchsine respectively for such comparison experiment. The results demonstrated that the degradation velocity of Degussa P25 titania is slow at the initial stage, and gradually increases with time (Figure 13a). In contrast, the photocatalytic degradation velocity of branched CdS nanowires is very quick at the primary stage, which can be ascribed to rapid adsorption of acid fuchsine on the branched nanostructures, then degrading gradually with time (Figure 13b). When time is prolonged up to 150 min, the acid fuchsine almost completely degraded with the branched CdS nanowires but a small amount of acid fuchsine still exists in the case of Degussa P25 titania (Figure 13). Generally, the branched CdS nanowire photocatalyst shows much greater activity than that of Degussa P25.

Conclusions

Semiconductor CdS and CdSe nanostructures with complex form such as urchin-like nanoflowers, branched nanowires, and fractal nanotrees can be synthesized via a facile solvothermal approach in a mixed solution made of diethylenetriamine (DETA) and deionized water (DIW). The results demonstrated that the morphologies of CdS and CdSe nanocrystals can be controlled via tuning the volume ratio of DETA and DIW. This facile solvothermal reaction in a mixed solution can access a variety of semiconductor nanomaterials with complex form. These nanomaterials can be produced in substantial amounts and exhibit more effective photocatalytic performance compared to that of Degussa P25 titania, as demonstrated in the photodegradation of acid fuchsine at ambient temperature. The results suggested that the photocatalytic property of CdS nanostructures is related to its unique structural feature.

Acknowledgment. S.H.Y. thanks the funding support from the Centurial Program of the Chinese Academy of Sciences, the National Science Foundation of China (Nos. 20325104, 20321101, and 50372065), and the Scientific Research Foundation for the Returned Overseas Chinese Scholars supported by the State Education Ministry, the Specialized Research Fund for the Doctoral Program (SRFDP) of Higher Education State Education Ministry, and the Partner-Group of the Chinese Academy of Sciences-the Max Planck Society.

Supporting Information Available: FE-SEM images and XPS spectra of products prepared at 180 °C for 12 h and FE-SEM images of CdSe nanostructures. This material is available free of charge via the Internet at http://pubs.acs.org.

References and Notes

(1) (a) Mcclean, I. P.; Thomas, C. B. *Semicond. Sci. Technol.* **1992**, *7*, 1394. (b) Deshmuhk, I. P.; Holikatti, S. G.; Hankare, P. P. *J. Phys. D: Appl. Phys.* **1996**, *27*, 1784. (c) Peng, X.; Schlamp, M. C.; Kadavanich, A. V.; Alivisatos, A. P. *J. Am. Chem. Soc.* **1997**, *119*, 7019. (d) Wang, Z. L. *Adv. Mater.* **2000**, *12*, 1295. (e) Duan, X. F.; Huang, Y.; Agarwal, R.; Lieber, C. M. *Nature* **2003**, *421*, 241. (f) Agarwal, R.; Barrelet, C. J.; Lieber, C. M. *Nano Lett.* **2005**, *5*, 917. (g) Barrelet, C. J.; Greytak, A. B.; Lieber, C. M. *Nano Lett.* **2004**, *4*, 1981. (h) Liu, Y. K.; Zapien, J. A.; Geng, C. Y.; Shan, Y. Y.; Lee, C. S.; Lifshitz, Y.; Lee, S. T. *Appl. Phys. Lett.* **2004**, *85*, 3241.

(2) (a) Milliron, D. J.; Hughes, S. M.; Cui, Y.; Manna, L.; Li, J. B.; Wang, L. W.; Alivisatos, A. P. *Nature* **2004**, *430*, 190. (b) Yu, W. W.; Qu, L. H.; Guo, W. Z.; Peng, X. G. *Chem. Mater.* **2003**, *15*, 2854. (c) Yu, W. W.; Peng, X. G. *Angew. Chem., Int. Ed.* **2002**, *41*, 2368. (d) Peng, Z. A.; Peng, X. G. *J. Am. Chem. Soc.* **2001**, *123*, 183. (e) Cao, Y. C.; Wang, J. H. *J. Am. Chem. Soc.* **2004**, *126*, 14336. (f) Pan, D. C.; Jiang, S. C.; An, L. J.; Jiang, B. Z. *Adv. Mater.* **2004**, *16*, 982. (g) Chen, M.; Xie, Y.; Lu, J.; Xiong, Y. J.; Zhang, S. Y.; Qian, Y. T.; Liu, X. M. *J. Mater. Chem.* **2002**, *12*, 748. (h) Pinna, N.; Weiss, K.; Sack-Kongehl, H.; Vogel, W.; Urban, J.; Pileni, M. P. *Langmuir* **2001**, *17*, 7982. (i) Pinna, N.; Weiss, K.; Urban, J.; Pileni, M. P. *Adv. Mater.* **2001**, *13*, 261. (j) Bekele, H.; Fendler, J. H.; Kelly, J. W. *J. Am. Chem. Soc.* **1999**, *121*, 7266. (k) Lazell, M.; O'Brien, P. *J. Mater. Chem.* **1999**, *9*, 1381. (l) Matsumoto, H.; Sakata, T.; Mori, H.; Yoneyama, H. *J. Phys. Chem.* **1996**, *100*, 13781. (m) Korgel, B. A.; Monbouquette, H. G. *J. Phys. Chem.* **1996**, *100*, 346.

(3) (a) Liang, H. J.; Angelini, T. E.; Braun, P. V.; Wong, G. C. L. *J. Am. Chem. Soc.* **2004**, *126*, 14157. (b) Dong, L. F.; Gushtyuk, T.; Jiao, J. *J. Phys. Chem. B* **2004**, *108*, 1617. (c) Li, Y. C.; Li, X. H.; Yang, C. H.; Li, Y. F. *J. Mater. Chem.* **2003**, *13*, 2641. (d) Mang, P.; Gao, L. *Langmuir* **2003**, *19*, 208. (e) Yang, C. S.; Awschalom, D. D.; Stucky, G. D. *Chem. Mater.* **2002**, *14*, 1277. (f) Nair, P. S.; Radhakrishnan, T.; Revaprasadu, N.; Kolawole, G. A.; O'Brien, P. *Chem. Commun.* **2002**, 564. (g) Gao, F.; Lu, Q. Y.; Xie, S. H.; Zhao, D. Y. *Adv. Mater.* **2002**, *14*, 1537. (h) Jun, Y. W.; Lee, S. M.; Kang, N. J.; Cheon, J. *J. Am. Chem. Soc.* **2001**, *123*, 5150.

(4) (a) Ge, J. P.; Li, Y. D. *Adv. Funct. Mater.* **2004**, *14*, 157. (b) Wang, Y. W.; Meng, G. W.; Zhang, L. D.; Liang, C. H.; Zhang, J. *Chem. Mater.* **2002**, *14*, 1773. (c) Ye, C. H.; Meng, G. W.; Wang, Y. H.; Jiang, Z.; Zhang, L. D. *J. Phys. Chem. B* **2002**, *106*, 10338. (d) Wang, Y. W.; Meng, G. W.; Zhang, L. D.; Liang, C. H.; Zhang, J. *Chem. Mater.* **2002**, *14*, 1773. (e) Cao, H. Q.; Xu, Y.; Hong, J. M.; Liu, H. B.; Yin, G.; Li, B. L.; Tie, C. Y.; Xu, Z. *Adv. Mater.* **2001**, *13*, 1393. (f) Zhan, J. H.; Yang, X. G.; Wang, D. W.; Li, S. D.; Xie, Y.; Xia, Y. N.; Qian, Y. T. *Adv. Mater.* **2000**, *12*, 1348. (g) Yan, P.; Xie, Y.; Qian, Y. T.; Liu, X. M. *Chem. Commun.* **1999**, 1293.

(5) (a) Xiong, Y. J.; Xie, Y.; Yang, J.; Zhang, R.; Wu, C. Z.; Du, G. *J. Mater. Chem.* **2002**, *12*, 3712. (b) Shao, M. W.; Xu, F.; Peng, Y. Y.; Wu, J.; Li, Q.; Zhang, S. Y.; Qian, Y. T. *New J. Chem.* **2002**, *26*, 1440. (c) Peng, T. Y.; Yang, H. P.; Dai, K.; Pu, X. L.; Hirao, K. *Chem. Phys. Lett.* **2003**, *379*, 432. (d) Rao, C. N. R.; Govindaraj, A.; Deepak, F. L.; Gunari, N. A.; Nath, M. *Appl. Phys. Lett.* **2001**, *78*, 1853.

(6) (a) Gao, T.; Wang, T. H. *J. Phys. Chem. B* **2004**, *108*, 20045. (b) Ip, K. M.; Wang, C. R.; Li, Q.; Hark, S. K. *Appl. Phys. Lett.* **2004**, *84*, 795. (c) Zhang, J.; Jiang, F. H.; Zhang, L. D. *J. Phys. Chem. B* **2004**, *108*, 7002. (d) Dong, L. F.; Jiao, J.; Coulter, M.; Love, L. *Chem. Phys. Lett.* **2003**, *376*, 653.

(7) (a) Li, Y. D.; Liao, H. W.; Ding, Y.; Qian, Y. T.; Yang, L.; Zhou, G. E. *Chem. Mater.* **1998**, *10*, 2301. (b) Peng, Q.; Dong, Y. J.; Deng, Z. X.; Li, Y. D. *Inorg. Chem.* **2002**, *41*, 5249. (c) Deng, Z. X.; Li, L. B.; Li, Y. D. *Inorg. Chem.* **2003**, *42*, 2331. (d) Yang, J.; Zeng, J. H.; Yu, S. H.; Yang, L.; Zhou, G. E.; Qian, Y. T. *Chem. Mater.* **2000**, *12*, 3259. (e) Yu, S. H.; Wu, Y. S.; Yang, J.; Han, Z. H.; Xie, Y.; Qian, Y. T.; Liu, X. M. *Chem. Mater.* **1998**, *10*, 2309. (f) Yu, S. H.; Yoshimura, M.; Moreno, J. M. C.; Fujiwara, T.; Fujino, T.; Teranishi, R. *Langmuir* **2001**, *17*, 1700.

(8) Wang, D.; Lieber, C. M. *Nature Mater.* **2003**, *2*, 355.

(9) (a) Manna, L.; Milliron, D. J.; Meisel, A.; Scher, E. C.; Alivisatos, A. P. *Nature Mater.* **2003**, *2*, 382. (b) Gao, P.; Wang, Z. L. *J. Phys. Chem. B* **2002**, *106*, 12653. (c) Lao, J.; Wen, J.; Ren, Z. F. *Nano Lett.* **2002**, *2*, 1287. (d) Yan, H.; He, R.; Johnson, J.; Law, M.; Saykally, R. J.; Yang, P. *J. Am. Chem. Soc.* **2003**, *125*, 4728.

(10) Brust, M.; Walker, M.; Bethell, D.; Schiffrin, D. J.; Whyman, R. *J. Chem. Soc., Chem. Commun.* **1994**, *7*, 801.

(11) Pan, D. C.; Jiang, S. C.; An, L. J.; Jiang, B. Z. *Adv. Mater.* **2004**, *16*, 982.

(12) Yao, W. T.; Yu, S. H.; Pan, L.; Li, J.; Wu, Q. S.; Zhang, L.; Jiang, J. *Small* **2005**, *1*, 320.

(13) Yao, W. T.; Yu, S. H.; Jiang, J.; Zhang, L. *Chem. Eur. J.* **2006**, *12*, 2066.

(14) Yao, W. T.; Yu, S. H.; Huang, X. Y.; Jiang, J.; Zhao, L. Q. X.; Pan, L.; Li, J. *Adv. Mater.* **2005**, *17*, 2799.

(15) Kanaras, A. G.; Sonnichsen, C.; Liu, H. T.; Alivisatos, A. P. *Nano Lett.* **2005**, *5*, 2164.

(16) (a) Witten T. A., Jr.; Sander, L. M. *Phys. Rev. Lett.* **1981**, *47*, 1400. (b) Meakin, P. *Phys. Rev. A* **1983**, *27*, 1495. (c) Halsey, T. C.; Duplantier, B.; Honda, K. *Phys. Rev. Lett.* **1997**, *78*, 1719.

(17) Ming, N. B.; Wang, M.; Peng, R. W. *Phys. Rev. B* **1993**, *48*, 621.

(18) (a) Milliron, D. J.; Hughes, S. M.; Cui, Y.; Manna, L.; Li, J. B.; Wang, L. W.; Alivisatos, A. P. *Nature* **2004**, *430*, 190. (b) Manna, L.; Scher, E. C.; Alivisatos, A. P. *J. Am. Chem. Soc.* **2000**, *122*, 12700.

(19) (a) Duxin, N.; Liu, F. T.; Vali, H.; Eisenberg, A. *J. Am. Chem. Soc.* **2005**, *127*, 10063. (b) Zhao, H.; Douglas, E. P. *Chem. Mater.* **2002**, *14*, 1418. (c) Spanhel, L.; Haase, M.; Weller, H.; Henglein, A. *J. Am. Chem. Soc.* **1987**, *109*, 5649.

(20) (a) Shriagami, T.; Fukami, S.; Wada, Y.; Yanagida, S. *J. Phys. Chem.* **1993**, *97*, 12882. (b) Torimoto, T.; Maeda, K.; Maenaka, J.; Yoneyama, H. *J. Phys. Chem.* **1994**, *98*, 13658. (c) Fujiwara, H.; Hosokawa, H.; Murakoshi, K.; Wada, Y.; Yanagida, S.; Okada, T.; Kobayashi, H. *J. Phys. Chem. B* **1997**, *101*, 8270. (d) Hirai, T.; Bando, Y.; Komasawa, I. *J. Phys. Chem. B* **2002**, *106*, 8967.

(21) (a) Fox, M. A.; Dulay, M. T. *Chem. Rev.* **1993**, *93*, 341. (b) Kabra, K.; Chaudhary, R.; Sawhney, R. L. *Ind. Eng. Chem. Res.* **2004**, *43*, 7683. (c) Tsuji, I.; Kato, H.; Kudo, A. *Angew. Chem., Int. Ed.* **2005**, *44*, 3565. (d) Guo, Y.; Zhang, H.; Wang, Y.; Liao, Z. L.; Li, G. D.; Chen, J. S. *J. Phys. Chem. B* **2005**, *109*, 21602. (e) Wang, S. M.; Liu, P.; Wang, X. X.; Fu, X. Z. *Langmuir* **2005**, *21*, 11969.

(22) Hu, J. S.; Ren, L. L.; Guo, Y. G.; Liang, P. L.; Cao, A. M.; Wan, L. J.; Bai, C. L. *Angew. Chem., Int. Ed.* **2005**, *44*, 1269.